TISSUE ENGINEERING: Part A
Volume 17, Numbers 3 and 4, 2011

DOI: 10.1089/ten.tea.2010.0274

Elastomeric Osteoconductive Synthetic Scaffolds with Acquired Osteoinductivity Expedite the Repair of Critical Femoral Defects in Rats

Tera M. Filion, B.S.,[1,2] Xinning Li, M.D.,[1] April Mason-Savas, B.S.,[1] Jaclynn M. Kreider, M.S.,[3] Steven A. Goldstein, Ph.D.,[3] David C. Ayers, M.D.,[1] and Jie Song, Ph.D.[1,2]

Regenerative medicine aspires to reduce reliance on or overcome limitations associated with donor tissue-mediated repair. Structural bone allografts are commonly used in orthopedic surgery, with a high percentage of graft failure due to poor tissue integration. This problem is aggravated among elderly, those suffering from metabolic conditions, or those undergoing cancer therapies that compromise graft healing. Toward this end, we developed a synthetic graft named FlexBone, in which nanocrystalline hydroxyapatite (50 wt%) was structurally integrated with crosslinked poly(hydroxyethyl methacrylate) hydrogel, which provides dimensional stability and elasticity. It recapitulates the essential role of nanocrystalline hydroxyapatite in defining the osteoconductivity and biochemical microenvironment of bone because of its affinity for biomolecules. Here, we demonstrate that FlexBone effectively absorbed endogenously secreted signaling molecules associated with the inflammation/graft healing cascade upon being press-fit into a 5-mm rat femoral segmental defect. Further, when preabsorbed with a single dose of 400 ng recombinant human (rh) bone morphogenetic protein-2/7 heterodimer, it enabled the functional repair of the critical-sized defect by 8–12 weeks. FlexBone was stably encapsulated by the bridging bony callus and the FlexBone–callus interface was continuously remodeled. In summary, FlexBone combines the dimensional stability and osteoconductivity of structural bone allografts with desirable surgical compressibility and acquired osteoinductivity in an easy-to-fabricate and scalable synthetic biomaterial.

Introduction

Synthetic scaffolds designed to assist tissue repair should exhibit useful surgical handling characteristics, a biochemical microenvironment promoting proper cellular response and tissue integration, and structural/chemical properties ensuring long-term stability and safety. Synthetic bone substitutes currently in clinical use (e.g., brittle ceramics, weak polymer gel foams) rarely possess essential bone-like structural and biochemical properties. In addition, they often lack desirable physical properties that would facilitate convenient surgical insertion and stable graft fixation and/or they generate immunogenic/inflammatory degradation products *in vivo*. Although new and exciting biomaterial scaffolds incorporating sophisticated chemical and engineering designs have been recently reported in literature, they continue to present major hurdles, slowing their bench-to-bedside translation.[1]

We believe that the sophisticated functional requirements of a viable synthetic bone graft are not synonymous with complicated materials designs. Instead, we propose that the recapitulation of the multifaceted roles of nanocrystalline hydroxyapatite (nHA), the key mineral component of bone, as part of a strategy for the design of a synthetic scaffold will lead to a successful bone graft substitute. Toward this end, we developed FlexBone, a structural composite with up to 50 wt% nHA structurally integrated within a hydroxylated crosslinked carbon network.[2] Despite its high mineral content, this structural composite can withstand repetitive functional-compressive loads with excellent shape recovery under physiological conditions.[2] As a result of the high surface area of the nHA component and its intrinsic affinity for proteins and small molecule therapeutics,[3,4] FlexBone is also a suitable vehicle for delivering growth factors and antibiotics in a sustained and localized manner *in vitro* (Supplementary Fig. S1; Supplementary Data are available online at www.liebertonline.com/ten).[5] Further, FlexBone can be predrilled with interconnecting channels to enable the migration of endogenous progenitor cells upon implantation. Combined with its ease of preparation in large scale, safe storage under ambient conditions, and the ability to be supplemented with osteogenic protein therapeutics at the

Departments of [1]Orthopaedics and Physical Rehabilitation and [2]Cell Biology, University of Massachusetts Medical School, Worcester, Massachusetts.
[3]Department of Orthopaedic Surgery, University of Michigan, Ann Arbor, Michigan.

time of use, FlexBone has the potential to be an "off-the-shelf" synthetic bone substitute for orthopedic applications. In this study, we test the hypothesis that the elasticity, osteoconductivity, and dimensional stability exhibited by FlexBone, combined with its osteoinductivity acquired from preabsorbed recombinant human bone morphogenetic protein-2/7 heterodimer (rhBMP-2/7), makes it an effective scaffold in enabling the functional repair of critical femoral defects in rats.

As will be described, we utilized a 5-mm rat femoral segmental defect model[6] to evaluate the efficacy of FlexBone comprising two mineral compositions, 50 wt% nHA (FB-50), or 25 wt% nHA plus 25 wt% tricalcium phosphate (TCP) (FB-25-25). In addition, we also delivered the heterodimer BMP-2/7 via FlexBone to facilitate the repair. BMP-2 and BMP-7 are both Food and Drug Administration-approved protein therapeutics for promoting skeletal repair.[7] BMP-2 plays a critical role in initiating fracture healing[8] and is clinically used for tibial fractures and spinal fusions. BMP-7 may play a larger role in the later stages of bony repair[9–11] and is routinely used for spinal fusions and nonunions. It has been also used in revision surgeries following inadequate repairs by BMP-2 treatment. BMP-2/7 heterodimer was shown to be a more potent osteogenic factor than either homodimer *in vitro*[12] and can be used at a lower effective concentration.[13] In this study, we use the rhBMP-2/7 heterodimer to augment the osteointegration and graft healing of FlexBone.

Methods

Graft preparation

FlexBone with two mineral compositions, 50 wt% nHA (FB-50) or 25 wt% nHA-25 wt% TCP (FB-25-25), were prepared to examine the potential impact of the faster dissolution of TCP[14] on graft remodeling. FB-50 and FB-25-25 were prepared as previously described.[2] Briefly, freshly distilled 2-(hydoxyethl methacrylate) (HEMA) was mixed with ethylene glycol dimethacrylate (EGDMA) along with ethylene glycol (EG), water, and aqueous radical initiators ammonium persulfate (I-1, 480 mg/mL) and sodium metasulfite (I-2, 180 mg/mL) at a volume ratio of HEMA:EGDMA:EG:I-1:I-2 of 100:2:35:20:5:5. Nanocrystalline HA powder was then added to the hydrogel mixture, thoroughly mixed, and allowed to polymerize in rigid acrylic tubing of an inner diameter of 3.2 mm (United States Plastic Corp.; tubes were washed with absolute ethanol to remove radical inhibitors and air-dried prior to use). The retrieved cylindrical FlexBone was cut into segments of ~5.5 mm in length and drilled with two intersecting orthogonal drill holes (a longitudinal channel, 1.19 mm in diameter, and an orthogonal channel, 0.79 mm in diameter, as illustrated in Fig. 1A) to allow bone marrow access upon implantation. FlexBone was then thoroughly equilibrated in MilliQ water to remove residual radical initiators, unreacted monomers, ethylene glycol, and debris from the drilling. After being sterilized with 70% ethanol, FlexBone was re-equilibrated with sterile water and dried for storage. Prior to surgical implantation, FlexBone was hydrated with saline for ~0.5 h (Supplementary Fig. S2) before an additional 8 μL saline or reconstituted rhBMP-2/7 solution (R&D Systems) was uniformly applied to give a final loading dose of 0 or 400 ng rhBMP-2/7 per graft.

Study design and surgical procedure

A 5-mm rat femoral segmental defect model[6] (Fig. 1B) was chosen to evaluate FlexBone-mediated skeletal repair as a function of mineral composition and osteogenic growth factor delivery. Four groups of FlexBone grafts (FB-50 and FB-25-25, with or without 400 ng rhBMP-2/7) were press-fit in 5-mm rat femoral defects, and the osteointegration of the grafts were examined over time. A no-graft control group was used to ensure the nonhealing nature of the 5-mm defect without graft treatment. The rats were euthanized at 4 days, 2, 4, 6, 8, and 12 weeks for histological examination. In a

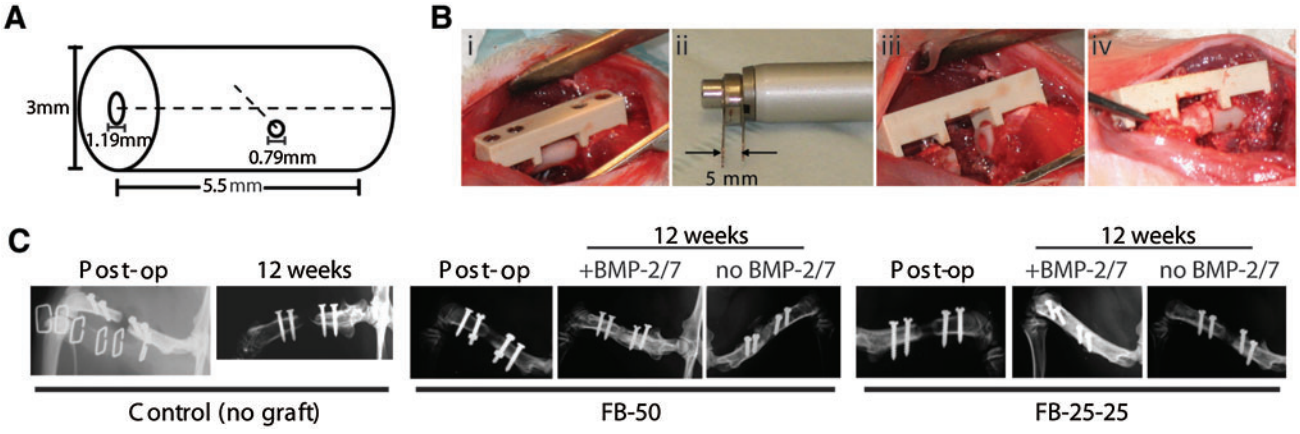

FIG. 1. Graft design **(A)**, surgical procedure **(B)**, and radiographic follow-ups **(C)**. The femoral segmental defect was surgically created by (i) securing a radiolucent polyetheretherketone (PEEK) plate fixator to the exposed femur (the periosteum was circumferentially removed from the femur to which the PEEK plate was attached with bicortical screws); (ii, iii) generating 5-mm middiaphyseal defect under the plate fixator with an oscillating Hall saw with parallel blades; and (iv) press-fitting a 5.5-mm long FlexBone (with or without 400 ng BMP-2/7) into the defect. Radiographic follow-ups confirmed the alignment and stability of the press-fit graft and the formation of a healing callus over 12 weeks. FB-50, FlexBone with 50 wt% nanocrystalline hydroxyapatite; FB-25-25, FlexBone with 25 wt% nanocrystalline hydroxyapatite plus 25 wt% tricalcium phosphate; BMP-2/7, bone morphogenetic protein-2/7 heterodimer. Color images available online at www.liebertonline.com/ten.

subset of 8- and 12-week rats, fresh frozen explanted femurs were evaluated by microcomputed tomography (microCT) and then tested to failure in torsion. To assess the role of the nHA in retaining endogenous proteins on FlexBone (see *Detection for endogenous proteins absorbed on FlexBone* section), additional FB-50 grafts and unmineralized poly (2-hydoxyethyl methacrylate) (pHEMA) control grafts were press-fit into 5-mm defects and retrieved at 0.5 h, 1 day, 2 days, 4 days, and 1 week for immunohistological analysis. A total of 160 defects were generated: 5 groups (FB-50 alone + FB-25-25 alone + FB-50 with BMP + FB25-25 with BMP + 1 no-graft control)×[6 time points×3 ($N=3$, histology) + 2 time points×5 ($N=5$, MicroCT and torsion test)] + 2 groups (FB-50 alone + unmineralized pHEMA control)×5 time points×2 ($N=2$, detection of endogenous proteins) = 160 defects. Finally, four intact femurs were collected for torsion from healthy unoperated rats that were of the same age as the rats receiving the grafts for 12 weeks.

All animal procedures were approved by the University of Massachusetts Medical School Animal Care and Use Committee. Briefly, sedated male Charles River SASCO-SD rats (289–300 g) were maintained by 2% isoflurane–oxygen throughout the surgery. The shaft of a femur was exposed by a combination of sharp and blunt dissections and the periosteum of the exposed femur was circumferentially removed to emulate a challenging clinical scenario where this important source of progenitor cells and signaling molecules is lost. A radiolucent, weight-bearing polyetheretherketone (PEEK) internal fixation plate was secured to the exposed femur with four bicortical screws into predrilled holes. A 5-mm middiaphyseal defect was then created using an oscillating Hall saw with parallel blades (Fig. 1B). The defect site was thoroughly irrigated with saline to remove bone debris and residue of detached periosteum before it was press-fit with a FlexBone graft with or without 400 ng rhBMP-2/7. The wounds were closed with sutures and the rats were given cefazolin (20 mg/kg) and bupenorphine (0.08 mg/kg) injections subcutaneously over the next 2 days. Rats were radiographed post-op to ensure proper graft positioning, and every 2 weeks thereafter to monitor the mineralized callus formation over time. On dates of scheduled explant retrieval, rats were sacrificed by isoflurane and cervical dislocation. The repaired femur, with the PEEK plate fixator intact, was carefully separated from the adjacent hip and knee joints by an oscillating saw.

Histology and microscopy

To evaluate cellularity, new bone formation, remodeling, and vascularization of the FlexBone over time, histochemical and immunohistochemical staining of the explants for hematoxylin and eosin, osteogenic differentiation marker alkaline phosphatase (ALP), osteoclast lineage marker tartrate-resistant acid phosphatase (TRAP), and chondrocytes (by toluidine blue) was performed on 6-μm paraffin sections. All explanted femurs were fixed in a periodate–lysine–paraformaldehyde fixative[15] at 4°C for 2 days and decalcified in 18% ethylenediaminetetraacetic acid (0.1 M Tris, pH 7.0) at 4°C for 4 weeks before they were bisected longitudinally for paraffin embedment and sectioning. Polarized light microscopy was used to assess the orientation of collagen fibrils and thus the maturity of new bone formation.

Detection of endogenous proteins absorbed on FlexBone

FB-50 grafts and unmineralized pHEMA controls were press-fit into the 5-mm critical-sized rat femoral defects in a subset of experiments. The grafts were harvested and fixed at 0.5 h, 1 day, 2 days, 4 days, and 1 week, during which the inflammatory/graft healing cascade was initiated. Antibodies for transforming growth factor β (TGFβ) (detects precursor and mature TGFβ1, 2, and 3 isoforms; Santa Cruz), tumor necrosis factor α (Novus Biologicals), interleukin-1β (Santa Cruz), vascular endothelial growth factor (Santa Cruz), receptor activator for nuclear factor kappa B ligand (RANKL) (Abcam), BMP-2 (Novus Biologicals), BMP-7 (Abcam), and stromal cell-derived factor (SDF)-1 (Santa Cruz) were used to detect the endogenous proteins absorbed on FB-50 and pHEMA at each time point. Unimplanted FB-50 were stained for the same panel of antibodies and immunoglobulin G isotype (rabbit or mouse immunoglobulin G) control stains were performed on all FB-50 explants retrieved at various time points (Supplementary Information; Supplementary Fig. S4). For the TGFβ detection, positive control stain was performed on a FB-50 graft loaded with 10 ng rhTGFβ1 (R&D Systems), and negative control stain using the blocking peptide (Santa Cruz) along with the primary antibody was also carried out. The immunohistochemical detection was performed on paraffin-embedded sections as described above.

MicroCT and biomechanical tests

Fresh-frozen explants were scanned on a cone-beam eXplore Locus SP microCT system. The effective voxel size of the reconstructed images was $18\times18\times18\,\mu m^3$. Images were globally thresholded and analyzed to measure callus volume and bone mineral content. Both ends of the same explants were then potted in aluminum pots with molten bismuth and mounted in a custom minitorsion tester. PEEK fixators were carefully bisected using a high-speed burr under irrigation before the explants were loaded to failure (0.5°/s), to determine failure torque and energy to failure.

Statistical analyses

The Wilcoxon–Mann–Whitney ranked-sum test was used to make all statistical comparisons and p-values <0.05 were considered significant. All analyses were performed using STATA (version 9.0) software.

Results

Partial healing of femoral critical defects by FlexBone in the absence of exogenous growth factors

Elastomeric FlexBone grafts of either mineral composition, predrilled with two intersecting orthogonal channels for marrow penetrations (Fig. 1A), were readily press-fit into the 5-mm defects with excellent alignment to adjacent bones (Fig. 1B). Radiographic monitoring of the graft healing by X-ray (Fig. 1C) showed that the grafts remained stably positioned throughout the study, with calcified callus partially or completely bridging over the defect by 12 weeks.

Histological analyses and polarized light microscopy (Fig. 2) revealed that the osteoconductivity of FlexBone facilitated healing in the absence of exogenous osteogenic

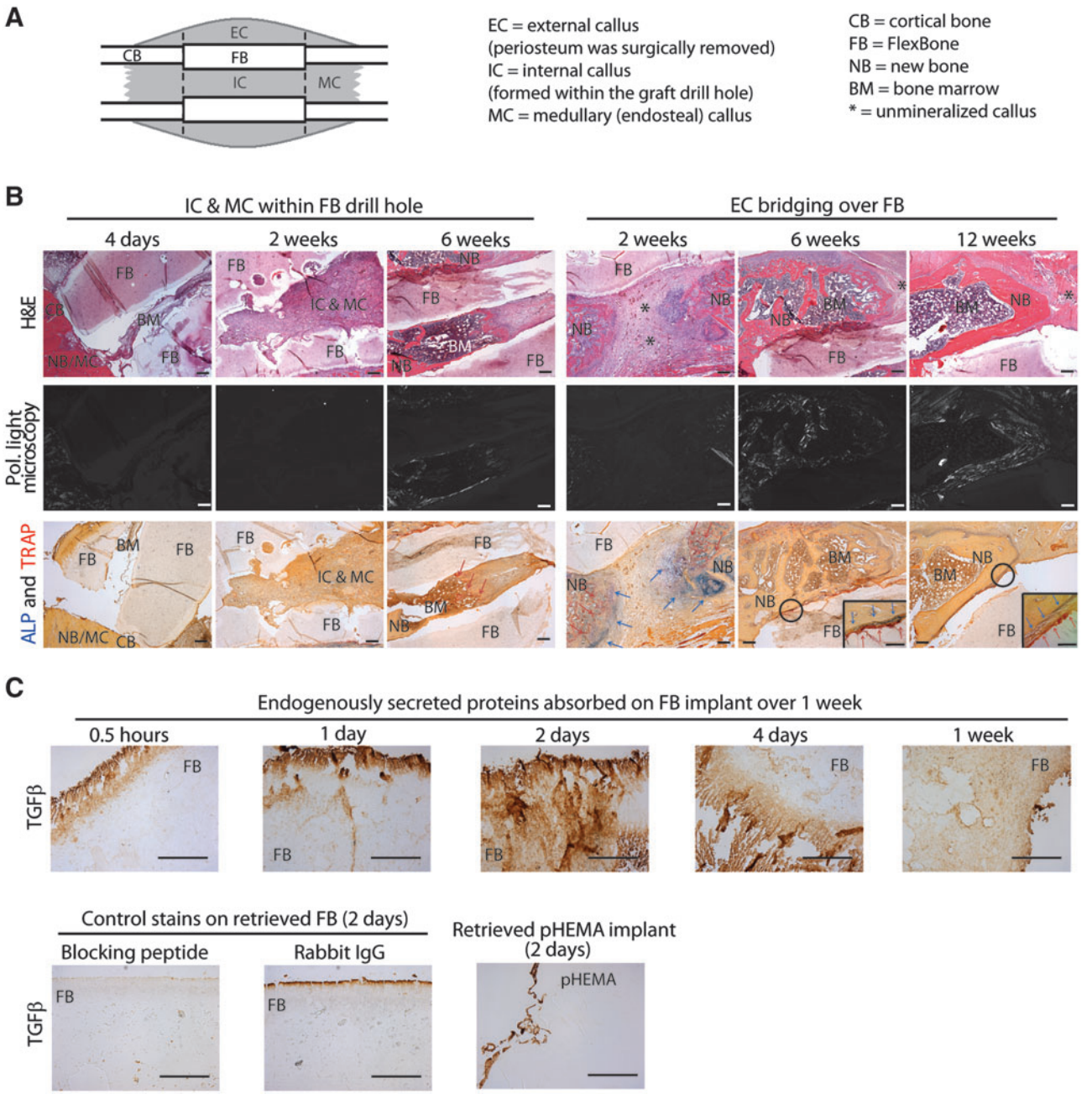

FIG. 2. Cartoon depiction **(A)**, histological analyses **(B)** of the callus formation surrounding a femoral segmental defect fit with FB-50 without recombinant human (rh) BMP-2/7, and immunohistological detection **(C)** of endogenous proteins absorbed on FB-50. Longitudinal sections of the explants obtained at various time points were stained for H&E, ALP (blue), and TRAP (red) to assess the cellularity and tissue types and to monitor osteoblastic and osteoclastic activities within the healing callus. Polarized light microscopy was used to assess collagen fibril orientation within the callus. Panel **C** selectively shows the absorption of endogenous TGFβ (see Supplementary Fig. S4 for a panel of additional proteins) on FB-50 within 1 week of implantation in rat femoral defects. Negative control stains of the 2-day FB-50 explant using TGFβ blocking peptide and rabbit IgG isotype control, respectively, are selectively shown. Endogenous TGFβ detected on pHEMA retrieved on day 2 is representatively shown (see Supplementary Fig. S4 for other time points). Scale bars = 200 μm. H&E, hematoxylin and eosin; ALP, alkaline phosphatase; TRAP, tartrate-resistant acid phosphatase; TGFβ, transforming growth factor β; pHEMA, poly (2-hydoxyethyl methacrylate).

growth factors. Bone marrow penetration throughout the orthogonal drill holes of the graft (FB-50), the emergence of an external callus, and the formation of an internal/medullary callus (within the graft drill hole and adjacent medullary cavity; Fig. 2A) were evident at 4 days post-op (Fig. 2B). By 2 weeks, the external callus bridging over the defect was partially mineralized, with ossification extending from the graft–cortical bone interfaces toward the center of the callus. Cartilage, stained purple by toluidine blue (Supplementary Fig. S3), was prominently present at the mineralizing ends of

the external callus, underscoring the endochondral ossification mechanism. By 6 weeks, both the external and internal calluses were significantly remodeled and matured as evidenced by the recanalization[16] and the formation of oriented collagen fibrils revealed by polarized microscopy.[17] Although even greater orientation of collagen fibrils within the external callus was observed beyond 6 weeks, bridging of the defect by fully mineralized callus was not achieved by 12 weeks without rhBMP-2/7.

Remodeling activity (indicated by positive ALP and TRAP stains) was detected within internal, external, and medullary calluses throughout the 12-week study. A line of osteoclastic activity (red TRAP stain) was typically observed at the FlexBone–callus interface, followed by a distinct line of osteoblastic activity (blue ALP stain), suggesting coordinated remodeling and osteointegration of FlexBone. Quantification of the numbers of TRAP-positive cell nuclei and ALP-positive cell nuclei at the graft–callus interface over time (Supplementary Table S1) revealed persisting active graft remodeling activities by 6 weeks as evidenced by the increased osteoclastic activities compared with those detected at 2 weeks. Intense TRAP and ALP stains were still detected at the FlexBone–callus interface at 12 weeks, suggesting that graft remodeling would continue over an extended period of time. Histological analysis of the FB-25-25 graft healing over time revealed similar observations.

In a subset of experiments (Supplementary Fig. S4), we showed that FlexBone effectively absorbed a number of endogenously secreted factors (TGFβ, interleukin-1β, tumor necrosis factor α, vascular endothelial growth factor, RANKL, BMP-2, BMP-7, and SDF-1) associated with the initiation of the inflammation[18,19]/graft healing cascade[20] and the recruitment of progenitor cells.[21,22] The majority of these factors were initially (0.5 h after implantation) detected on the surface of the graft where progenitor cells were recruited to, and then the secreted molecules quickly penetrated throughout the three-dimensional network and were effectively retained by the nHA component (Fig. 2C). In contrast, the unmineralized pHEMA controls were not able to attract and retain these endogenously secreted molecules within its three-dimensional network.

Expedited healing of femoral critical defects by FlexBone in the presence of rhBMP-2/7

Acceleration of graft healing by delivery of rhBMP-2/7 using FlexBone was examined with each mineral composition. The capacity of FlexBone to locally deliver exogenous rhBMP-2/7 enhanced the graft osteoinductivity and led to expedited repair of the critical-sized femoral defects by 8 weeks (Fig. 3). When press-fit with FlexBone (FB-50) containing 400 ng rhBMP-2/7, the defect was completely bridged by maturing and recanalizing internal and external bony calluses at 6 weeks. By 8 weeks, the collagen fibrils in the healing calluses exhibited excellent alignment with little change observed beyond that point. FB-25-25 supplemented with 400 ng rhBMP-2/7 enabled the formation of bridging bony calluses in a similar fashion. The accelerated active graft remodeling in the presence of rhBMP-2/7 was evidenced by >50% higher counts of TRAP-positive cell nuclei at 2 weeks post-op, and a more rapid drop of the number by 6 weeks when compared with those observed for the group without BMP-2/7 treatment (Supplementary Table S1).

Quantitative assessment of the repair of femoral critical defects by FlexBone as a function of mineral composition and rhBMP-2/7 treatment

Quantitative assessment of the healing callus formation by microCT (Fig. 4A) and torsion testing (Fig. 4B) indicated successful functional repair of the critical-sized femoral defects by 12 weeks using FlexBone augmented with 400 ng rhBMP-2/7. Three-dimensional reconstruction of the mi-

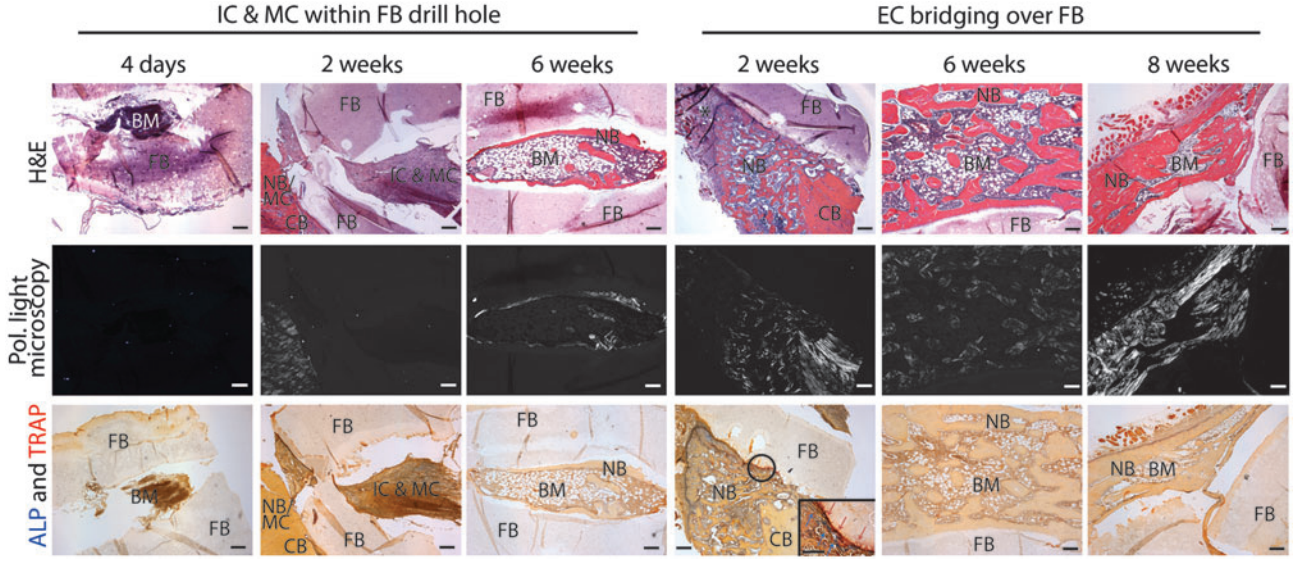

FIG. 3. Histological analyses of the callus formation surrounding a femoral segmental defect fit with FB-50 with recombinant human (rh) BMP-2/7 (400 ng). Longitudinal sections of the explants obtained at various time points were stained for H&E, ALP (blue), and TRAP (red) to assess the cellularity and tissue types and to monitor osteoblastic and osteoclastic activities within the healing callus. Polarized light microscopy was used to assess collagen fibril orientation within the callus. Scale bars = 200 μm.

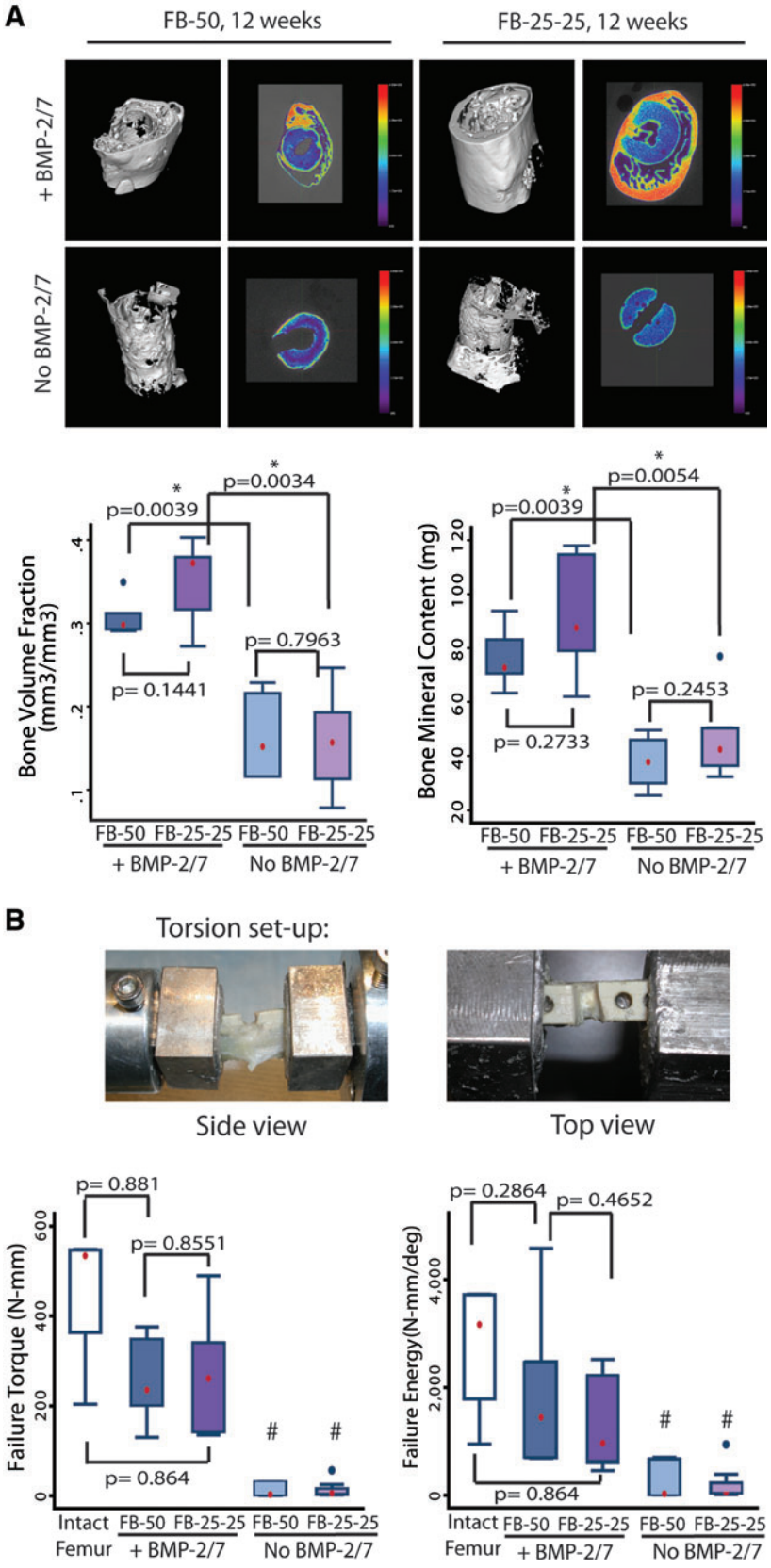

FIG. 4. Microcomputed tomography analyses **(A)** and torsion tests **(B)** of 12-week explants as a function of graft mineral composition and BMP-2/7 treatment. Effective voxel size of $18\times18\times18$ μm^3 was applied to the reconstructed three-dimensional isosurface images and the two-dimensional color maps of the center slice of the explants (red representing a higher degree of mineralization). Graphed data are presented as boxplots, where red dots indicate median values and blue dots represent sample outliers. Note that FB explants without BMP-2/7 treatment did not fail during the torsion test (likely due to the lack of a fully bridging stiff bony callus and the elasticity of underlying FlexBone). #The values reported represent the torque and energy at which the testing was stopped. *$p < 0.05$ is considered significant. Color images available online at www.liebertonline.com/ten.

croCT scans revealed robust mineralized external callus completely bridging over the FlexBone-filled defects when supplemented with rhBMP-2/7. Two-dimensional color maps of the center cross-sections confirmed that the midpoint of these grafts was fully encapsulated with mature and recanalized external and internal mineralized calluses. In contrast, defects filled by FlexBone of either mineral composition without rhBMP-2/7 treatment were only partially bridged by mineralized calluses. With the treatment of a single dose of 400 ng BMP-2/7, bone volume fractions and bone mineral contents of the 12-week explants increased by >100%. From 8 to 12 weeks post-op, defects treated with FB-50 and rhBMP-2/7 showed little increase in bone mineral content (Supplementary Fig. S5B) but a 20% increase in bone volume fraction (Supplementary Fig. S5A), suggesting continued remodeling of the bony callus beyond 8 weeks.

The remarkable healing achieved by a combination of osteogenesis and osteoconduction in the growth factor–treated group translated into the restoration of torsional strength of the femoral defects. The maximum torque and energy to failure values of the explants in the rhBMP-2/7–treated group approximate those of intact femurs (Fig. 4B),[23] or the femoral defects repaired by gene therapy,[20,24] and surpass those accomplished by allograft-mediated repair.[25] Despite an upward trend over time, the observed difference in failure torque or failure energy between the 8- and 12-week explants was statistically insignificant (Supplementary Fig. S5C, D), suggesting that the bony callus formed at 8 weeks already possessed adequate strength.

Discussion

We have shown that FlexBone, a structural composite of nHA and hydrophilic pHEMA hydrogel matrix, possessed unique properties desired for the repair of critical-sized femoral defects. The elasticity of FlexBone allowed for its convenient and stable press-fitting into a critical-sized femoral defect, which was stabilized by a weight-bearing fixation plate. Predrilled interconnected channels facilitated bone marrow penetration and enabled the stabilization of the defect via the formation of both internal and external calluses. Effective recruitment of bone marrow progenitor cells via the drill holes and the affinity of the nHA component for endogenously secreted signals required for initiating the inflammation/graft healing cascade are likely contributors to the partial repair enabled by FlexBone in the absence of any exogenous osteogenic factor.

Further, we demonstrate that the local delivery of low-dose rhBMP-2/7 via FlexBone (400 ng/graft) enabled expedited functional repair of the critical defect by 8–12 weeks via its acquired osteoinductivity. The biomechanical function of the defect was restored to the level comparable to those achieved by successful gene therapy, but without the common risks associated with the latter.[20,24] This was likely due to the robust host-to-host junction of the bridging bony callus, the increase in cross-sectional area (callus volume), and the degree of mineralization of the new bone collar. The low rhBMP-2/7 working dose accomplished in this study is 1–2 orders of magnitude lower than those utilized in the rhBMP-2 therapy in treating similar defects,[26,27] likely resulting from a combination of higher potency of the heterodimer and the ability of FlexBone to release it in a more sustained and localized manner.[5] This feature could be translated into FlexBone-mediated delivery of protein therapeutics in a more cost-effective and safer fashion (e.g., with less proteins rapidly diffused away from the carrier), potentially benefiting the clinical treatment of hard-to-heal bony lesions.

No significant difference in the functional outcome (based on microCT and torsion data) of FlexBone-assisted repair of critical femoral defects was observed by 12 weeks between the two mineral compositions examined (FB-50 vs. FB-25-25). To fully reveal the impact of the different dissolution rates of TCP versus nHA on graft remodeling, detailed microstructural analyses of the healing callus over a longer period of time would be necessary. The choice for mineral composition will likely be dictated by the desired physical properties of the scaffold for any given application. For instance, FB-25-25 has higher compressability than FB-50 under physiological conditions, achieving 25% strain (as opposed to 10% for FB-50[5]) under 0.5 MPa compressive load,[2] making it easier to be press-fit into a defect with limited accessibility. The stiffer properties of the FB-50, on the other hand, could enable the graft more tightly fit within an open defect.

The dimensional stability and biocompatibility of FlexBone, along with the persistent remodeling observed at the graft–callus interface, resemble some of the best features of structural allografts.[28] Patients receiving a successful structural allograft implantation would often live with the allograft for life, with the graft being slowly remodeled over time, generating little inflammatory degradation product. Unlike the overwhelming numbers of biodegradable polymeric bone substitutes designed for tissue engineering applications,[29] the crosslinked pHEMA hydrogel network in FlexBone is not hydrolytically degradable by design. Vital organs collected from the rats receiving FlexBone implants for 12 weeks were pathologically indistinguishable from age-matched control organs harvested from unoperated rats (Supplementary Fig. S6). We argue that biodegradability is not a functional requirement of viable synthetic bone grafts. However, to further explore the clinical potential of FlexBone, *in vivo* studies using large animal models and full toxicological analyses for determining the longer-term remodeling pattern and safety (longer-term systemic effects) of FlexBone need to be carried out.

In summary, FlexBone combines some of the best features of structural allografts (osteoconductivity and dimensional stability)[29–31] with desirable surgical compressibility and scalability of synthetic biomaterials. The ability of FlexBone to locally deliver biological therapeutics in a significantly reduced effective dose to enable expedited functional repair of the critical defect opens the door to engineer the biochemical properties of the graft[21] based on individual needs. More broadly, our work supports the notion that functional sophistication of synthetic tissue grafts is not synonymous with complicated chemical/engineering designs.[1] We show that by recapitulating the multifaceted roles that key extracellular matrix components play in defining tissue-specific microenvironment, easy-to-prepare biomaterials can be designed to facilitate functional tissue repair.

Acknowledgments

This work was supported by the National Institutes of Health grants 5R01AR055615 (to J.S.) and 5P30DK32520, the

American Society for Bone and Mineral Research Career Enhancement Award (to J.S.), and the Orthopaedic Research and Education Foundation Resident Clinician Scientist Training Grant (to X.L.). J. Song is a member of the UMASS Diabetes Endocrinology Research Center (DK32520). The authors thank James Potts for advising on the statistical analyses.

Disclosure Statement

No competing financial interests exist.

References

1. Place, E.S., Evans, N.D., and Stevens, M.M. Complexity in biomaterials for tissue engineering. Nat Mater **8,** 457, 2009.
2. Song, J., Xu, J., Filion, T., Saiz, E., Tomsia, A.P., Lian, J.B., Stein, G.S., Ayers, D.C., and Bertozzi, C.R. Elastomeric high-mineral content hydrogel-hydroxyapatite composites for orthopedic applications. J Biomed Mater Res A **89,** 1098, 2009.
3. Gilbert, M., Shaw, W.J., Long, J.R., Nelson, K., Drobny, G.P., Giachelli, C.M., and Stayton, P.S. Chimeric peptides of statherin and osteopontin that bind hydroxyapatite and mediate cell adhesion. J Biol Chem **275,** 16213, 2000.
4. Stubbs, J.T., 3rd, Mintz, K.P., Eanes, E.D., Torchia, D.A., and Fisher, L.W. Characterization of native and recombinant bone sialoprotein: delineation of the mineral-binding and cell adhesion domains and structural analysis of the RGD domain. J Bone Miner Res **12,** 1210, 1997.
5. Xu, J., Li, X., Lian, J.B., Ayers, D.C., and Song, J. Sustained and localized *in vitro* release of BMP-2/7, RANKL, and tetracycline from FlexBone, an elastomeric osteoconductive bone substitute. J Orthop Res **27,** 1306, 2009.
6. Fang, J.M., Zhu, Y.Y., Smiley, E., Bonadio, J., Rouleau, J.P., Goldstein, S.A., McCauley, L.K., Davidson, B.L., and Roessler, B.J. Stimulation of new bone formation by direct transfer of osteogenic plasmid genes. Proc Natl Acad Sci USA **93,** 5753, 1996.
7. Gautschi, O.P., Frey, S.P., and Zellweger, R. Bone morphogenetic proteins in clinical applications. ANZ J Surg **77,** 626, 2007.
8. Tsuji, K., Bandyopadhyay, A., Harfe, B.D., Cox, K., Kakar, S., Gerstenfeld, L., Einhorn, T., Tabin, C.J., and Rosen, V. BMP2 activity, although dispensable for bone formation, is required for the initiation of fracture healing. Nat Genet **38,** 1424, 2006.
9. White, A.P., Vaccaro, A.R., Hall, J.A., Whang, P.G., Friel, B.C., and McKee, M.D. Clinical applications of BMP-7/OP-1 in fractures, nonunions and spinal fusion. Int Orthop **31,** 735, 2007.
10. Wang, F.S., Yang, K.D., Kuo, Y.R., Wang, C.J., Sheen-Chen, S.M., Huang, H.C., and Chen, Y.J. Temporal and spatial expression of bone morphogenetic proteins in extracorporeal shock wave-promoted healing of segmental defect. Bone **32,** 387, 2003.
11. Onishi, T., Ishidou, Y., Nagamine, T., Yone, K., Imamura, T., Kato, M., Sampath, T.K., ten Dijke, P., and Sakou, T. Distinct and overlapping patterns of localization of bone morphogenetic protein (BMP) family members and a BMP type II receptor during fracture healing in rats. Bone **22,** 605, 1998.
12. Israel, D.I., Nove, J., Kerns, K.M., Kaufman, R.J., Rosen, V., Cox, K.A., and Wozney, J.M. Heterodimeric bone morphogenetic proteins show enhanced activity *in vitro* and *in vivo*. Growth Factors **13,** 291, 1996.
13. Zheng, Y., Wu, G., Zhao, J., Wang, L., Sun, P., and Gu, Z. rhBMP2/7 heterodimer: an osteoblastogenesis inducer of not higher potency but lower effective concentration compared with rhBMP2 and rhBMP7 homodimers. Tissue Eng Part A **16,** 879, 2010.
14. Tang, R.K., Wu, W.J., Haas, M., and Nancollas, G.H. Kinetics of dissolution of beta-tricalcium phosphate. Langmuir **17,** 3480, 2001.
15. Miao, D., and Scutt, A. Histochemical localization of alkaline phosphatase activity in decalcified bone and cartilage. J Histochem Cytochem **50,** 333, 2002.
16. Schell, H., Lienau, J., Epari, D.R., Seebeck, P., Exner, C., Muchow, S., Bragulla, H., Haas, N.P., and Duda, G.N. Osteoclastic activity begins early and increases over the course of bone healing. Bone **38,** 547, 2006.
17. Cool, S.M., Forwood, M.R., Campbell, P., and Bennett, M.B. Comparisons between bone and cementum compositions and the possible basis for their layered appearances. Bone **30,** 386, 2002.
18. Schindeler, A., McDonald, M.M., Bokko, P., and Little, D.G. Bone remodeling during fracture repair: the cellular picture. Semin Cell Dev Biol **19,** 459, 2008.
19. Einhorn, T.A. The cell and molecular biology of fracture healing. Clin Orthop Relat Res **(355 Suppl),** S7, 1998.
20. Lieberman, J.R., Daluiski, A., Stevenson, S., Wu, L., McAllister, P., Lee, Y.P., Kabo, J.M., Finerman, G.A., Berk, A.J., and Witte, O.N. The effect of regional gene therapy with bone morphogenetic protein-2-producing bone-marrow cells on the repair of segmental femoral defects in rats. J Bone Joint Surg Am **81,** 905, 1999.
21. Ito, H., Koefoed, M., Tiyapatanaputi, P., Gromov, K., Goater, J.J., Carmouche, J., Zhang, X.P., Rubery, P.T., Rabinowitz, J., Samulski, R.J., Nakamura, T., Soballe, K., O'Keefe, R.J., Boyce, B.F., and Schwarz, E.M. Remodeling of cortical bone allografts mediated by adherent rAAV-RANKL and VEGF gene therapy. Nat Med **11,** 291, 2005.
22. Kitaori, T., Ito, H., Schwarz, E.M., Tsutsumi, R., Yoshitomi, H., Oishi, S., Nakano, M., Fujii, N., Nagasawa, T., and Nakamura, T. Stromal cell-derived factor 1/CXCR4 signaling is critical for the recruitment of mesenchymal stem cells to the fracture site during skeletal repair in a mouse model. Arthritis Rheum **60,** 813, 2009.
23. Kidder, L.S., Chen, X., Schmidt, A.H., and Lew, W.D. Osteogenic protein-1 overcomes inhibition of fracture healing in the diabetic rat: a pilot study. Clin Orthop Relat Res **467,** 3249, 2009.
24. Hsu, W.K., Sugiyama, O., Park, S.H., Conduah, A., Feeley, B.T., Liu, N.Q., Krenek, L., Virk, M.S., An, D.S., Chen, I.S., and Lieberman, J.R. Lentiviral-mediated BMP-2 gene transfer enhances healing of segmental femoral defects in rats. Bone **40,** 931, 2007.
25. Pelker, R.R., McKay, J., Jr., Troiano, N., Panjabi, M.M., and Friedlaender, G.E. Allograft incorporation: a biomechanical evaluation in a rat model. J Orthop Res **7,** 585, 1989.
26. Kirker-Head, C., Karageorgiou, V., Hofmann, S., Fajardo, R., Betz, O., Merkle, H.P., Hilbe, M., von Rechenberg, B., McCool, J., Abrahamsen, L., Nazarian, A., Cory, E., Curtis, M., Kaplan, D., and Meinel, L. BMP-silk composite matrices heal critically sized femoral defects. Bone **41,** 247, 2007.

27. Abarrategi, A., Moreno-Vicente, C., Ramos, V., Aranaz, I., Casado, J.V.S., and Lopez-Lacomba, J.L. Improvement of porous beta-TCP scaffolds with rhBMP-2 chitosan carrier film for bone tissue application. Tissue Eng Part A **14,** 1305, 2008.
28. Reynolds, D.G., Hock, C., Shaikh, S., Jacobson, J., Zhang, X., Rubery, P.T., Beck, C.A., O'Keefe, R.J., Lerner, A.L., Schwarz, E.M., and Awad, H.A. Micro-computed tomography prediction of biomechanical strength in murine structural bone grafts. J Biomech **40,** 3178, 2007.
29. Baroli, B. From natural bone grafts to tissue engineering therapeutics: brainstorming on pharmaceutical formulative requirements and challenges. J Pharm Sci **98,** 1317, 2009.
30. Blokhuis, T.J., and Lindner, T. Allograft and bone morphogenetic proteins: an overview. Injury **39 Suppl 2,** S33, 2008.
31. Goldberg, V.M., and Stevenson, S. Bone-graft options—fact and fancy. Orthopedics **17,** 809, 1994.

Address correspondence to:
Jie Song, Ph.D.
Department of Orthopedics
University of Massachusetts Medical School
55 Lake Avenue North
Worcester, MA 01655

E-mail: jie.song@umassmed.edu

Received: May 08, 2010
Accepted: September 03, 2010
Online Publication Date: October 15, 2010